Possibilities of combining radiant wall cooling with ejector cooling cycle powered by Fresnel solar collectors

Michal Krajčík[1,*], *Michal* Masaryk[2], *Martin* Šimko[1] and *Peter* Mlynár[2]

[1]Slovak University of Technology, Faculty of Civil Engineering, Radlinského 11, 81005 Bratislava, Slovakia
[2]Slovak University of Technology, Faculty of Mechanical Engineering, Námestie slobody 17, 81231 Bratislava, Slovakia

Abstract. Solar ejector cooling presents an alternative to the commonly used compressor vapour machines. It is a potentially feasible technology for space cooling providing that the temperature of the cooling water is high enough to assure reasonable efficiency of the chiller. This could be achieved by increasing the evaporation temperature of the cooling cycle through its combination with a high-temperature radiant cooling system. We explore the possibilities and benefits of combining a high-temperature radiant wall system with a solar ejector cycle for space cooling of buildings. The lowest water temperature in the wall to prevent condensation was 18°C for the wall with pipes underneath the surface whereas it was 14°C for the wall with pipes embedded in the thermal core. Thus, the evaporation temperature was substantially higher for the radiant systems than for fancoils. For the conventional vapour compressor cooling, this increased the system efficiency (COP) by 30 to 50%. The COP of the ejector cooling cycle was about half of that for the compressor vapour cycle when R1234ze was used as the refrigerant, however, the primary energy was lower for ejector cooling. Using thermally active building systems (TABS) provided a reasonable cool storage capacity for as much as five hours which allows turning the cooling machines off for several hours during peaks in energy demand.

1 Introduction

The dominant role of buildings as energy consumers and greenhouse gasses producers [1] has led the policymakers to reinforce the requirements on the energy efficiency of buildings in the recently approved EU directives. For example, the required share of renewable energy sources on the overall buildings' energy consumption is 32 % in 2030 [2], the CO_2 emission reduction is 80 to 95 % in 2050 as compared to the levels in 1990 [3], and the primary energy reduction is 32.5 % in 2030 [4].

The energy demand for cooling and its share on the energy use in buildings has been steadily increasing since the 1990s [5], partially because of the increasing share of modern buildings with a high amount of glazed areas. The main energy consumers in cooling systems are the cooling machines consuming electricity with a high primary energy factor. The energy performance of buildings can be therefore enhanced by improving the energy efficiency of space cooling systems.

Compressor chillers have been traditionally used to generate cool for the space cooling systems. The ejector cooling cycle, in which the role of compressor is assumed by an ejector nozzle, presents an alternative to the compressor vapour systems [6-8]. The most important advantage of the ejector cooling cycle over compressor chillers is the fact that it is powered by heat instead of electricity. This means that ejector cooling can be a very competitive technology providing that enough solar or industrial waste heat is available.

The ejector cooling system consists predominantly of three plate heat exchangers. The key component is the nozzle (ejector), where underpressure is established due to the Venturi effect. Due to the underpressure in the nozzle, the working fluid is sucked from the evaporator whereby a pressure difference is created. In classical compressor machines, this pressure is created by the compressor. Despite the efficiency of the ejector cooling cycle may be lower than that of the compressor vapour cycle, its major advantage is that the main driving force is heat instead of electrical power. Another advantage is that it can use water as the refrigerant with a significantly lower global warming potential than the commonly used halogen carbons.

The combination of ejector cooling with Fresnel collectors is an emerging technology that has the potential to significantly enhance the efficiency of cooling systems [9-11]. Fresnel collectors are composed of polished reflex plane mirrors that rotate around the horizontal axis and thereby track the location of the Sun in the sky and reflect the solar radiation to the absorber. The absorber is a glazed transparent evacuated tube, located under a reflective roof. Fresnel collectors can be preferable to the traditional solar collectors because they enable reaching higher driving temperatures. This increases the efficiency of the ejector cooling machines.

* Corresponding author: michal.krajcik@stuba.sk

The most important parameter affecting the efficiency of the cooling machine is the evaporation temperature of the refrigerant in the evaporator [12,13]. The higher the evaporation temperature, the higher is the efficiency of the cooling machine and the less energy needs to be delivered. From this point of view, using radiant systems can help improve system efficiency. Compared to all-air systems, radiant cooling needs a substantially higher water temperature to achieve the same sensible cooling capacity [14,15]. Another potential advantage of the radiant systems is the possibility to store cool in their thermal mass which would allow turning off the cooling aggregates during peak loads. The cool can be generated and stored during night time when the electricity price is lower than during the day [16-18]. It can also help prevent exceeding the maximum permissible electricity peak outputs.

Although research on radiant surfaces has mostly focused on structural floors and ceilings, evidence from several research studies suggests that radiant walls also present a potentially feasible solution [19-21]. Radiant walls are more efficient in terms of heat and cool emission than heated ceilings and cooled floors, respectively, and they have higher heating capacity per surface area than floor heating due to a wider range of permissible surface temperatures [22,23]. Moreover, wall systems can be more suitable for building retrofit [24,25] and have higher cooling capacity than floors [26].

In the present study, we consider two types of cooling machines used in cooling technology: (1) a commonly used compressor vapour cooling machine, and (2) a novel promising combination of ejector cooling powered by Fresnel solar collectors. The two types of cooling machines have been considered in combination with fancoils representing a conventional cool emission system and with three types of wall cooling systems which differ from each other by the configuration of their material layers and level of thermal mass. The objectives are defined as follows:

- Compare the water temperature, the potential of energy storage and thermal dynamics of the three wall cooling systems. This data will be used as inputs for the subsequent calculations of the efficiency of the cooling aggregates.
- Investigate the energy benefits of using solar ejector cooling as compared to the traditional compressor cooling.
- Determine the energy benefits of combining the cooling machines with a high-temperature wall cooling system instead of the conventionally used fancoils.

2 Water temperature and thermal dynamics of radiant wall cooling

2.1. Wall cooling systems studied

The three radiant wall cooling systems considered are shown in Fig. 1 and are described as follows:

Wall A has pipes embedded in a reinforced plaster between concrete core and thermal insulation. It can be used for new buildings or attached to facades of existing buildings as a part of their retrofit, without any significant intervention on the interior side.

Wall B has pipes embedded in the concrete core, which makes its installation realistic only in new buildings.

Wall C has the pipes thermally uncoupled from the concrete core by a layer of thermal insulation. It is potentially suitable for buildings retrofit.

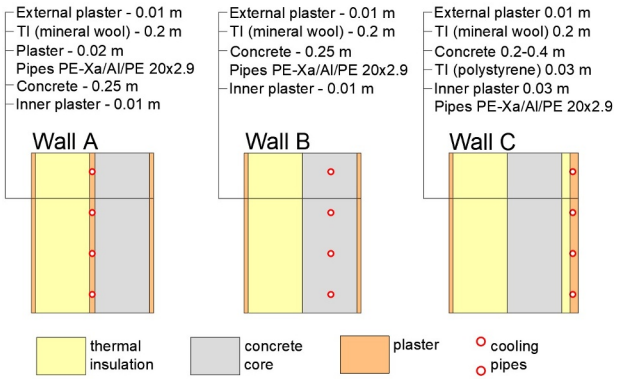

Fig. 1. Wall cooling systems studied.

2.2. Physical model and calculation method

The heat transfer was calculated by computer simulations for a characteristic wall fragment within a cooling wall. The computational model of Wall A was previously validated for summer [27]. The climatic conditions, simulation setup and solver in Ref. [27] were identical to those used in the present study. The geometry and thermo-physical properties of the material layers were slightly adjusted in the present study to make the system better suited for practical use. In the computational models of the other wall systems (B, C) the thermo-physical properties of the material layers, simulation setup, calculation procedure, and boundary conditions were identical with those for Wall A.

Stationary simulations were used to compute the cooling output and temperature distribution within the fragment, whereas dynamic simulations served to determine the thermal energy stored over time. The calculations were performed using CalA 3.2 software, which has been verified following EN ISO 10211 [28]. The software solves steady-state and dynamic 2D heat transfer by conduction:

$$\frac{\partial}{\partial x}\left(\lambda\frac{\partial T}{\partial x}\right)+\frac{\partial}{\partial y}\left(\lambda\frac{\partial T}{\partial y}\right)+S=\rho.c.\frac{\partial T}{\partial \tau} \quad (1)$$

where T is the temperature (K); S is an internal heat source (W/m^3); τ is time (s); λ is thermal conductivity (W/(m.K)); ρ is bulk density (kg/m^3); and c is the specific heat capacity at constant pressure (J/(kg.K)).

The heat was transferred to the environment through the surfaces facing the indoor and the outdoor environment. The other surfaces were assumed adiabatic. The specific heat flux on the inner and outer surface of a computational domain as well as on the pipe surface was calculated according to Robin-Newton's boundary condition. The simulation step used in the dynamic simulations was 15 minutes. The heat transfer coefficients on the inner and outer wall´s surface were 8 W/(m^2.K) and 15 W/(m^2.K), respectively. The calculation principle has been described in detail in [24,29].

The thermophysical properties of the individual material layers used in the calculation model are specified in Table 1. The thermal conductivity of the bearing structure can vary from very low typical, e.g., for aerated concrete or hollowed fire bricks to high typical, e.g., for reinforced concrete. In this study, the bearing structure is made of reinforced concrete because using this material for TABS is meaningful (Walls A and B). In all the simulations the thermo-physical properties of materials were considered constant, isotropic, and temperature independent.

Table 1. Thermo-physical properties of material layers.

Material	Thermal conductivity λ W/(m.K)	Specific heat capacity c J/(kg.K)
Inner plaster	0.7	840
Insulation - EPS F	0.04	1020
Reinforced concrete	1.58	1020
Insulation - mineral wool	0.04	940
Outer plaster	0.8	840
Plastic pipe ø 20	0.35	1000

The combined effect of ambient temperature and solar radiation incident on the wall was replaced by sol-air temperature ($T_{sol-air}$). The sol-air temperature can be interpreted as the outside air temperature which, in the absence of solar radiation, would give the same temperature distribution and rate of heat transfer through a wall as exists due to the combined effects of the actual outdoor temperature distribution plus the incident solar radiation [30].

The hourly and average values of ambient air temperature, the intensity of solar radiation and sol-air temperature for a design day realistic for the region of Central Europe are shown in Fig. 2. In the subsequent calculations, the sol-air temperature of 45 °C was used. A sensitivity analysis has shown that variations in sol-air temperature of several degrees Celsius have a negligible effect on the temperature distribution within the walls because of the thick thermal insulation.

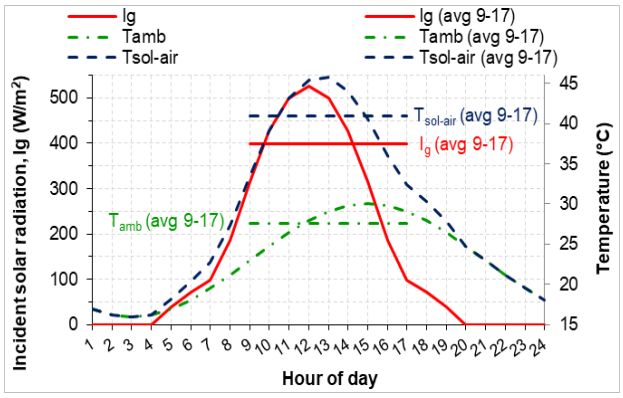

Fig. 2. The course of sol-air temperature, ambient temperature and intensity of solar radiation during the design day.

2.3. Surface temperature and dew point

Table 2 shows the effect of water temperature on the average and minimum surface temperature of the radiant cooling systems. The minimum water temperature is limited by the dew point temperature on the wall surface. For Walls A and B, the average surface temperature is identical with the minimum surface temperature, whereas for Wall C the difference is up to 2 K.

Table 2. The effect of water temperature on the surface temperature for the three wall cooling systems.

Temp. (°C)	Wall A			Wall B			Wall C		
T_{water}	8	10	12	12	14	16	16	18	20
$T_{surface,avg}$	20.7	21.3	21.9	18.6	19.7	20.7	20.6	21.6	22.8
$T_{surface,min}$	20.7	21.3	21.9	18.6	19.7	20.7	18.5	20.0	21.5

Key: T_{water} – water temperature, $T_{surface,avg}$ – average surface temperature, $T_{surface,min}$ – minimum surface temperature

Fig. 3 shows that at the room air temperature of 26 °C and relative humidity of 70 %, the limit on the minimum permissible surface temperature is about 20 °C. The water temperatures for Walls A and B, corresponding to the surface temperature of about 20 °C, are highlighted in green in Table 2. Although the dew point decreases with decreasing room air temperature and relative humidity, the 20 °C is considered as the safety limit to avoid condensation during typical operating conditions.

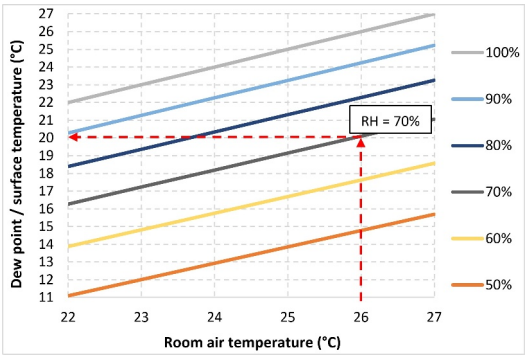

Fig. 3. Dew point temperature for various combinations of room air temperature and relative air humidity.

The detailed temperature fields in Fig. 4 support the understanding of the temperature distribution within the wall fragments (Table 2). It shows that Wall B needs a water temperature that is 4 K lower than that for Wall C to attain the same surface temperature of 20 °C. The water temperature needed for Wall A is so low that it is very close to water temperatures needed for fancoils. This system is therefore not considered in the subsequent calculations of the cooling system efficiency.

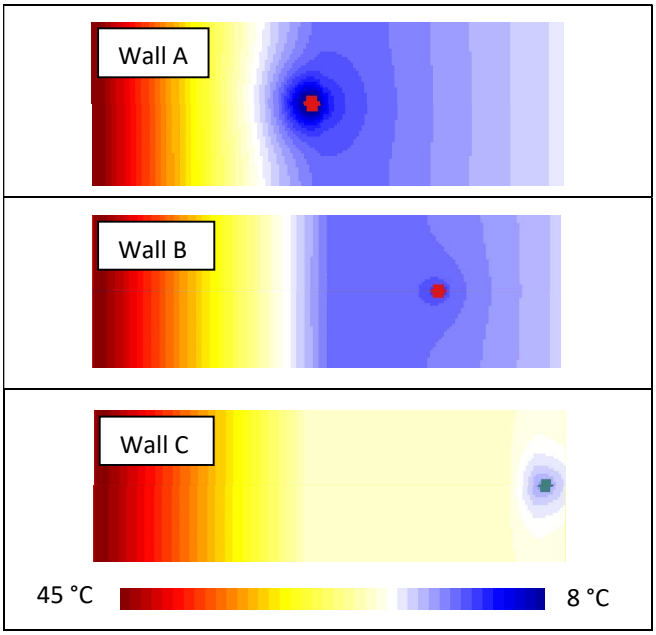

Fig. 4. Temperature distribution within wall fragments of the three wall cooling systems.

2.4. Water temperature and cooling output

Figs. 5 to 7 show the cooling output of the three wall systems for various areas of the cooling surface and the room temperature of 26 °C. For radiant heating and cooling systems, the cooling output is controlled by the "self-control" effect meaning that a small decrease in room temperature will significantly decrease the temperature difference between wall and space and thus the cooling output of the wall [31]. A sensitivity study has confirmed that for each of the wall cooling systems decreasing the room air temperature by 1 K reduces the cooling output by several W/m^2.

Figs. 5 and 6 show that for the cooling surface area of 50 m^2, the cooling output of Wall A at the water temperature of 8 °C corresponds to the cooling output of Wall B at 16 °C. The cooling output of Wall B at the water temperature of 16 °C corresponds to that of Wall C at 16 °C despite the pipe being very close to the surface in Wall C. This is because the temperature distribution throughout the surface of Wall C is not homogeneous. The surface of Wall C is cooler than the surface of Wall B close to the pipe but it is warmer than the surface of Wall B in between the pipes. Thus, the average surface temperature of the two systems is similar.

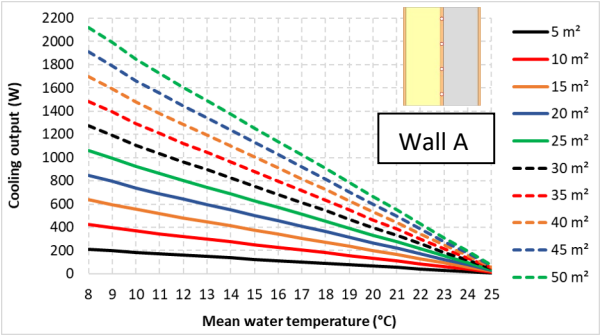

Fig. 5. Effect of water temperature on the cooling output at various cooling surface areas (Wall A).

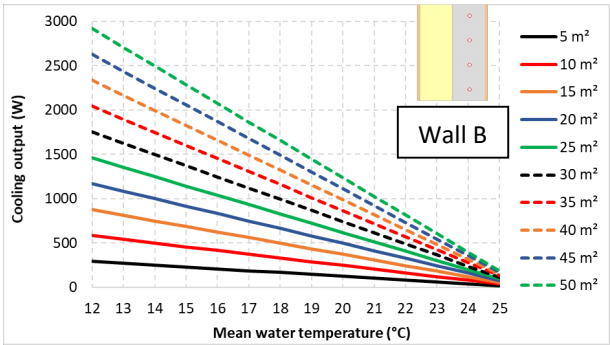

Fig. 6. Effect of water temperature on the cooling output at various cooling surface areas (Wall B).

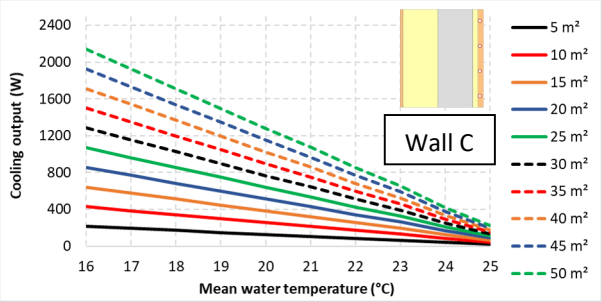

Fig. 7. Effect of water temperature on the cooling output at various cooling surface areas (Wall C).

2.5. Cooling energy stored

The cooling energy stored in the structure has been calculated by dynamic computer simulations for three realistic boundary conditions (Table 3). These conditions represent three levels of cooling load and the corresponding adjustment of the water temperature.

Figs. 8 to 10 show the substantial differences in cooling energy stored depending on the sol-air and water temperature and the wall cooling system investigated. At the water temperature of 14 °C, Wall B stores by 30 to 40 % more cooling energy than Wall A. This is caused by higher cooling losses and less homogeneous temperature distribution for Wall A. With Wall B, it is possible to accumulate about 800 Wh/m^2 over five hours and about 1200 Wh/m^2 over ten hours. This, in practice, means that the cool can be stored in the structure and the cooling machine can be turned off over several hours while the cool is being discharged.

Table 3. Boundary conditions used in the calculations of cooling energy stored.

Wall		Time	$T_{sol-air}$	T_{water}	T_{room}
A	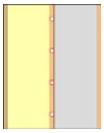	night	18	22	26
		morning	31	18	26
		afternoon	45	14	26
B	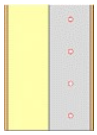	night	18	22	26
		morning	31	18	26
		afternoon	45	14	26
C	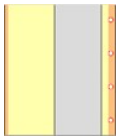	night	18	25	26
		morning	31	22	26
		afternoon	45	18	26

For Wall C the amount of energy stored is low and the rate of storage is too slow for utilization of the storage in practice. At the water temperature of 25 °C and the sol-air temperature of 18 °C the energy stored eventually becomes negative. This is because at the beginning of the dynamic simulation the structure had been already pre-cooled due to the sol-air temperature (18 °C) lower than the water (25 °C) and room (26 °C) temperature. The cooling energy stored in the structure before starting the simulations was being discharged to the interior, hence the negative values.

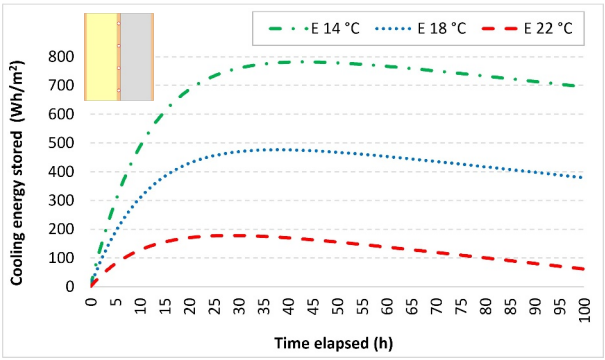

Fig. 8. Cooling energy stored at various water temperatures (Wall A).

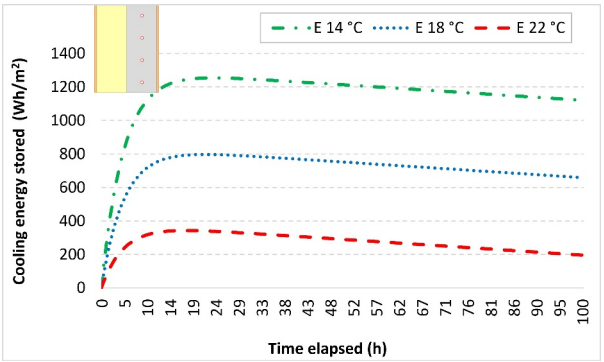

Fig. 9. Cooling energy stored at various water temperatures (Wall B).

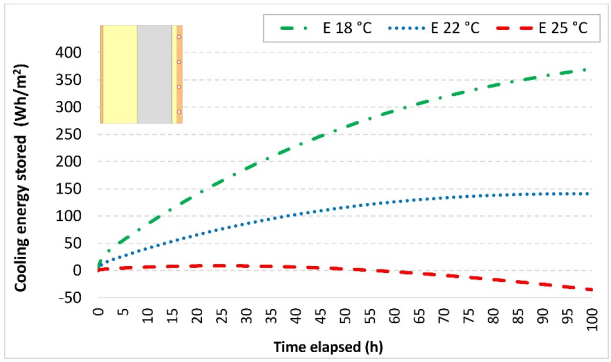

Fig. 10. Cooling energy stored at various water temperatures (Wall C).

3 Efficiency of compressor vapour cycle vs ejector cooling cycle

As shown in Table 2, two temperature levels of the cold distributing liquid are meaningful, 14 °C for Wall B (TABS) and 18 °C for Wall C. The evaporation temperature must be lower than the water temperature in the pipes in the wall that is subcooled in the evaporator. The evaporation temperatures in the evaporator were therefore set up three degrees lower to 11 °C and 15 °C. In a common technical solution with fancoils, where the air is cooled directly in the fancoils, the cooling water has to be subcooled down to 7 °C. The evaporation temperature, in this case, is therefore 3 °C. Thus, the efficiency of the cooling machines was compared in terms of COP for the evaporating temperatures of 3, 11, and 15 °C.

3.1. Compressor vapour cycle

A common Reversible Clausius-Rankine cooling vapour cycle was used for calculation, utilizing the log(p)-h diagram of the relevant refrigerants. Two new-generation refrigerants, R32 and R1234ze, as well as the commonly used R410A were considered. Although R410A has good thermodynamic characteristics, due to its negative environmental effects it is gradually being replaced by R1234ze. R1234ze is an ecological refrigerant and is suitable for use in vapour compressor as well as in ejector cooling cycles.

The efficiency of a compressor vapour cycle is expressed by the Coefficient of Performance (COP_{CC}) of the cooling machine:

$$COP_{CC} = Q_o / P_{el} \quad (2)$$

where Q_o is the cooling output and P_{el} is electric energy consumed by the compressor. Fig. 11 illustrates the effect of evaporation temperature on COP_{CC} for the refrigerant R410A. Electricity needed for the compressor is represented by the difference in enthalpy h_2-h_1, whereas the energy produced by the cooling machine is given by h_1-h_4. Increasing the evaporation temperature reduces the enthalpy difference h_2-h_1 whereby the COP_{CC} is enhanced.

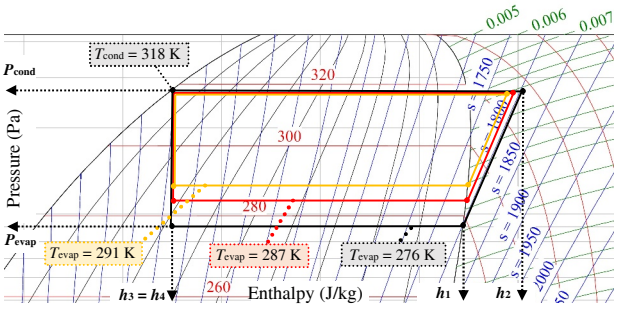

Fig. 11. Effect of evaporation temperature on enthalpy difference h_2-h_1 for R410A (log(p)-h diagram).

The COP_{CC} values for various evaporation temperatures are given in Table 4. The condensing temperature was set to 45 °C because it must be higher than the temperature of the environment. As shown in Table 4, higher evaporation temperatures result in a major increase in COP of the cooling machines, meaning a substantial reduction of energy consumption and operation costs.

Table 4. Efficiency of compressor vapour cycle (COP_{CC}) for various cool emission systems and refrigerants.

Refrigerant	Temp. (°C)	COP_{CC} (-)		
		R32	R410A	R1234ze
Condenser	45			
Evaporator (fancoil)	3	3.6	3.5	3.8
Evaporator (Wall B - TABS)	11	4.8	4.7	5.1
Evaporator (Wall C - pipes in plaster)	15	5.6	5.4	5.9

3.2. Ejector cooling cycle

Ejector cooling machines work under different conditions and partially also with different refrigerants than compressor vapour machines. Besides refrigerants like R1234ze, water can be used as a refrigerant in ejector cooling machines. Water presents a fully ecological refrigerant. However, at the boiling temperature of 3 °C its evaporation pressure is low, thus the conditions in the systems that use water are close to vacuum.

In solar ejector cooling, it is important using a lower condensing temperature to attain a reasonable efficiency of the cooling machine. A condensing temperature of 30 °C is realistic for solar cooling systems and was used in the calculation (Table 5). The high temperature needed in the generator to power the cooling machine is generated by the Fresnel solar collectors. The efficiency of the ejector cooling cycle, expressed by the Coefficient of Performance (COP_{EC}) of the cooling machine is given by:

$$COP_{EC} = Q_o / Q_{sol} \quad (3)$$

where Q_o is the cooling output and Q_{sol} is the solar energy supplied to the cooling machine from Fresnel solar collectors. In this case, the electricity needed for pumps is very small and was therefore neglected.

Table 5 shows that increasing the evaporator temperature substantially improves the COP_{EC} of the solar ejector cooling machine. Improving the COP_{EC} by using a high-temperature cooling system in practice means a smaller number of solar collectors needed to collect the heat for this kind of cooling machines. This results in a reduction of costs and the precious space needed for the installation of solar collectors.

Table 5. Efficiency of ejector cooling cycle (COP_{EC}) for various cool emission systems and refrigerants.

Refrigerant	water		R1234ze	
	Temp. (°C)	COP_{EC} (-)	Temp. (°C)	COP_{EC} (-)
Condenser	30		30	
Generator (powering)	150		100	
Evaporator (fancoil)	3	0.5	3	1.6
Evaporator (Wall B - TABS)	11	1.1	11	2.4
Evaporator (Wall C - pipes in plaster)	15	1.4	15	3.1

3.3. Effects on primary energy demand

Although the values of COP_{EC} obtained by solar ejector cooling are lower than those obtained by the vapour compressor cycle (COP_{CC}), the type of energy needed is qualitatively different. The compressor vapour cycle uses electricity, whereas the ejector cooling cycle uses solar energy to generate cool. The primary energy factor (PEF) of electricity is 2.2 in Slovakia, and it was determined to 2.67 for the EU-28 electricity generation mix based on data from 2015 [32]. The primary energy factor for concentrating solar power was estimated to 1.03 on the EU-level [32].

In energy calculations, the cooling demand is divided by the COP to obtain the amount of electricity needed to cover the cooling demand. To obtain the primary energy demand, the resulting number is multiplied by the primary energy factor. The primary energy coefficient of the cooling machine is represented by the ratio of primary energy factor to COP:

$$PE_{coeff} = \text{PEF} / \text{COP} \quad (4)$$

where COP is either COP_{CC} or COP_{EC}, depending on the type of cooling machine used.

At the same cooling demand, a lower primary coefficient indicates a lower primary energy demand of the cooling system. The primary energy coefficient of the compressor vapour cycle for the two alternative PEFs (Tables 6 and 7) can be compared with the primary energy coefficient of the ejector cooling cycle (Table 8). When using the refrigerant R1234ze, the primary energy coefficient is always lower for ejector cooling than for the compressor vapour cycle. Using radiant wall cooling significantly reduces the primary energy coefficient. In the ejector cooling cycle, the reduction is up to 50% for the combination with Wall C. Although water as a

refrigerant has lower COP and higher primary energy coefficients, it presents an alternative to the other refrigerants, with no negative effects on the environment.

Table 6. Primary energy coefficient for compressor vapour cycle, PEF = 2.2

Compressor vapour cycle (PEF = 2.2)			
	PEF / COP_{CC}		
Cooling system	**R32**	**R410A**	**R1234ze**
Fancoil	0.61	0.62	0.57
Wall B - TABS	0.46	0.47	0.43
Wall C - pipes in plaster	0.40	0.40	0.37

Table 7. Primary energy coefficient for compressor vapour cycle, PEF = 2.67

Compressor vapour cycle (PEF = 2.67)			
	PEF / COP_{CC}		
Cooling system	**R32**	**R410A**	**R1234ze**
Fancoil	0.73	0.75	0.70
Wall B - TABS	0.56	0.57	0.53
Wall C - pipes in plaster	0.48	0.49	0.45

Table 8. Primary energy coefficient for ejector cooling cycle

Ejector cooling cycle (PEF = 1.03)		
	PEF / COP_{EC}	
Cooling system	**water**	**R1234ze**
Fancoil	2.02	0.64
Wall B - TABS	0.90	0.42
Wall C - pipes in plaster	0.71	0.33

4 Conclusion

The possibilities and benefits of using a novel solar ejector cooling system instead of the traditional compressor vapour cooling have been investigated. Moreover, the effects of combining the cooling machine with high-temperature radiant cooling instead of fancoils representing a conventional solution have been studied.

The results indicate that by using high-temperature radiant cooling it is possible to attain a remarkable increase in the operation efficiency of cooling machines. This, in turn, reduces operation costs by lowering electricity consumption. For a conventional vapour compression cooling system the efficiency (COP) increases by 30 to 50 % depending on the temperature of the cooling water, whereas for the ejector cooling cycle combined with Fresnel solar collectors the efficiency (COP) doubles or even triples.

The thermal core of thermally active building systems (TABS) provides reasonable cool storage capacity for as much as five hours. This allows turning the cooling machines off for several hours during the expensive peaks in energy demand and also storing the cool during the night when the electricity prices are lower. Radiant systems with pipes located underneath the surface and decoupled from the main thermal mass are not suitable for energy storage but have a much shorter thermal response and are therefore much easier to control while providing a similar cooling output.

A comparison of the ejector cooling cycle with the compressor vapour cycle using R1234ze as a refrigerant has highlighted the potential of solar ejector cooling to reduce primary energy consumption. The efficiency was lower and primary energy was higher when water was used as a refrigerant. However, a suitable combination of high-temperature radiant system and solar ejector cooling with water as a refrigerant provides reasonable COP while significantly reducing the environmental impacts caused by the refrigerant.

This research was supported by the Slovak Research and Development Agency under contract No. APVV-16-0126 and Ministry of Education, Science, Research and Sport grant VEGA 1/0847/18.

References

1. International Energy Agency. Global Status Report – Towards a zero-emission, efficient and resilient buildings and construction sector (2018).
2. Directive (EU) 2018/2001 of the European Parliament and of the Council of 11 December 2018 on the promotion of the use of energy from renewable sources.
3. Directive 2012/27/EU of the European Parliament and of the Council of 25 October 2012 on energy efficiency, amending Directives 2009/125/EC and 2010/30/EU and repealing Directives 2004/8/EC and 2006/32/EC.
4. Directive (EU) 2018/2002 of the European Parliament and of the Council of 11 December 2018 amending Directive 2012/27/EU on energy efficiency.
5. IEA – International Energy Agency, https://www.iea.org/topics/energyefficiency/buildings/cooling/ (Accessed 18 May 2019).
6. Nguyen V.M., Riffat S.B. and Doherty P.S., 2001, Development of a solar-powered passive ejector cooling system, *Applied Thermal Engineering*, **21**, 157-168.
7. Varga S., Oliveira A.C., Diaconu B., 2009, Analysis of a solar-assisted ejector cooling system for air conditioning, *International Journal of Low-Carbon Technologies*, **4**, Issue 1, 2–8.
8. Rusly E., Aye L., Charters W.W.S. and Ooi A., 2005, CFD analysis of ejector in a combined ejector cooling system, *International Journal of Refrigeration*, **28**, Issue 7, 1092-1101.
9. Masaryk M. and Mlynár P., Solar-air-condition by ejector cooling, *AIP Conference Proceedings 2000*, 020013, 2018.
10. Sioud D., Raoudha G. and Bellagi A., 2018 Thermodynamic Analysis of a Solar Combined Ejector Absorption Cooling System, *Journal of Engineering*, 2018, 12 pages.

11. Bellos E., Tzivanidis Ch., 2017, Optimum design of a solar ejector refrigeration system for various operating scenarios, *Energy Conversion and Management*, **154**, 11-24.
12. Wang Z., Wang F., Wu X. and Tian Ch., 2016, Experimental investigation on dynamic performance of air-source heat pump water heater using R134a, *International Journal of Exergy (IJEX)*, **19**, No. 2.
13. Lecuona A., Ventas R., Venegas M., Zacarías A. and Salgado R., 2009, Optimum hot water temperature for absorption solar cooling, *Solar Energy*, **83**, 1806-1814.
14. Olesen B.W., 2008, Radiant floor cooling systems, *ASHRAE Journal*, **50**, Issue 9, 16-22.
15. Chicote M.A., Tejero A., Gómez E.V. and Rey F.J., 2012, Experimental study of the cooling capacity of a radiant cooled ceiling system, *Energy and Buildings*, **54**, 207–214.
16. B. Lehmann B., Dorer V. and Koschenz M., 2007, Application range of thermally activated building systems tabs, *Energy and Buildings*, **39**, 593‑598.
17. Schmelas M., Feldmann T., Wellnitz P. and Bollin E., 2016, Adaptive predictive control of thermo-active building systems (TABS) based on a multiple regression algorithm: first practical test, *Energy and Buildings*, **129**, 367‑377.
18. Koudelková D., 2018, Experimental measurement of the accumulated heat from the operation system of the heating in a building with a lightweight envelope, *Slovak Journal of Civil Engineering*, **26**, 65‑70.
19. Karabay H., Arici M. and Sandik M., 2013, A numerical investigation of fluid flow and heat transfer inside a room for floor heating and wall heating systems, *Energy and Buildings*, **67**, 471–478.
20. Myhren J.A. and Holmberg S., 2008, Flow patterns and thermal comfort in a room with panel, floor and wall heating, *Energy and Buildings*, **40**, 524–536.
21. Bojić M., Cvetković D., Marjanović V., Blagojević M. and Djordjević Z., 2013, Performances of low temperature radiant heating systems, *Energy and Buildings*, **61**, 233–238.
22. Romani J., Perez G. and de Gracia A., 2016, Experimental evaluation of a cooling radiant wall coupled to a ground heat exchanger, *Energy and Buildings*, **129**, 484–490.
23. Wang X., Zheng M., Zhang W., Zhang S. and Yang T., 2010, Experimental study of a solar-assisted ground coupled heat pump system with solar seasonal thermal storage in severe cold areas, *Energy and Buildings*, **42**, 2104–2110.
24. Krajcik M. and Sikula O., 2020, The possibilities and limitations of using radiant wall cooling in new and retrofitted existing buildings, *Applied Thermal Engineering*, 164, 114490.
25. Harmathy N., Urbancl D., Goričanec D. and Magyar Z., 2019, Energy efficiency and economic analysis of retrofit measures for single-family residential buildings, *Thermal Science*, **23**, No. 3B, 2071-2084.
26. Babiak J., Olesen B. W. and Petráš D., 2013, *Low temperature heating and high temperature cooling*, Rehva Guidebook No 7, 3rd revised ed., Rehva, Brussels.
27. M. Šimko, M. Krajčík, O. Šikula, Radiant wall cooling with pipes arranged in insulation panels attached to facades of existing buildings, *Proc. of the 13th REHVA World Congress Clima 2019*, Bucharest, Romania.
28. EN ISO 10211:2008, Thermal bridges in building construction. Heat flows and surface temperatures, Detailed calculations.
29. Šikula O., 2011, *Software CalA User Manual* (In Czech), Tribun, Brno, p. 42.
30. O´Callaghan P.W. and Probert S.D., 1977, Sol-air temperature, *Applied Energy*, **3**, 307‑311.
31. Olesen, B.W., 2002, Radiant floor heating in theory and practice, *ASHRAE Journal*, **7**, 19-24.
32. Fritsche U. and Greß W., 2015, *Development of the Primary Energy Factor of Electricity Generation in the EU-28 from 2010-2013*, International Institute for Sustainability Analysis and Strategy, Darmstadt.